

Vibrating Wire Station for Horizontal and Vertical Profiling of Proton Beam of Cyclotron C18 in Air

M. A. Aginian^a, A. P. Aprahamian^a, S. G. Arutunian^a, G. S. Harutyunyan^a, E. G. Lazareva^a*, L. M. Lazarev^a, A. V. Margaryan^a, L. A. Shahinyan^a, R. K. Dallakyan^a, A. A. Manukyan^a, V. K. Elbakyan^a, G. A. Hovhannisyan^a, G. E. Elbakyan^a, M. Chung^b, and D. Kwak^b

^a Alikhanyan National Science Laboratory, Yerevan, Armenia

^b Ulsan National Institute of Science and Technology, Ulsan, South Korea

*e-mail: ella.lazareva@yerphi.am

Received September 1, 2021; revised September 19, 2021; accepted September 26, 2021

Abstract—The paper presents the results of the first experiments on measuring the horizontal and vertical profiles of the proton beam of the C18 cyclotron using a profiling station based on vibrating wire monitors. The measurements were performed at the proton beam exit into the air from a special vacuum window located at the end of the cyclotron beam guide. The profiles were measured for different values of proton beam current. The station showed its operability under the conditions of strong disturbances caused by the exposure of protective lead plates to the proton beam.

Keywords: cyclotron, proton, beam, vibrating wire, profile

DOI: 10.3103/S1068337221040022

1. INTRODUCTION

Cyclotron C18 [1] is designed routinely for the production of medical isotopes such as ¹⁸F, ¹¹C, ¹³N, etc. [2]. The cyclotron is installed at the CJSC Isotope Production Center [3]. For the needs of the experimenters of the Yerevan Physics Institute, the beam is extracted into the experimental hall. For this purpose, a beamline is equipped by ending in a vacuum window through which the proton beam is moved into the air. For users of the extracted proton beam, the information about its exact location and the distribution of beam particles in its cross-section is essential. To measure the horizontal and vertical profiles of the beam, we have manufactured a beam profiling station, which consists of two vibrating wire monitors (VWM) equipped with linear drives based on stepper motors. Testing of the station was carried out using laser beams.

The station was installed directly behind the vacuum window of the cyclotron. The beam was scanned in the horizontal and vertical directions. A significant effect of the beam on the bearing parts of the monitors was found, in particular, on the lead screen installed on the front of the monitor to protect it from radiation during scanning. This exposure resulted in the heating of the lead plate and other parts of the monitors with a long time delay because of the thermal inertia of the massive parts of the sensor. By processing the obtained data, the horizontal and vertical profiles of the beam were reconstructed for various currents of the cyclotron.

2. CYCLOTRON C18

The C18 cyclotron of the Belgian company IBA was installed at the Radioisotope Production Center in 2014 and launched in 2019. Cyclotron C18 is a proton accelerator (H^+) with a fixed beam energy of 18 MeV. The maximum beam intensity is 150 μA . The cyclotron is equipped with 8 independent outputs, to which 8 different target modules or other equipment can be connected; the proton beam can be split (with the same energy) and taken out in parallel from two outputs. Negative ions are produced in the center of the device by two internal sources. Ions move in a magnetic field and are accelerated in an alternating high-frequency field on a pair of dees (see, for example, [4]). At the extraction radius, the ions, passing through a thin carbon foil, lose their electrons [5]. The resulting positive ions (protons) are bent outward towards the outputs by a magnetic field. The IBA has developed an innovative extraction method that allows one

to obtain the same size and properties of the extracted beam on the target window, regardless of the target number. This is achieved because of the correct design and shape of the magnet poles [6]. This procedure allows one to extract more than 99.9% of the accelerated beam [5].

2.1. Vacuum Window for the C18 Cyclotron

Nuclear physics is one of the promising experimental directions of the Yerevan Physics Institute [7, 8]. The problems of low-energy nuclear physics at the LUE-75 accelerator are discussed, for example, in [9, 10].

The C18 cyclotron is also planned for use by employees of the Yerevan Physics Institute in experiments in the field of nuclear physics (see, for example, [11–14]), where the possibility of producing technetium-99m using the proton beam of the cyclotron was noted. For this purpose, when designing the cyclotron building, an experimental hall with a beam guide for beam extraction was provided. A target module for solid targets NIRTA SOLID TARGET MODULE was attached to the end of the beamline in the factory configuration [15, 16]. In June 2020, a vacuum window was developed and created in the Production and Isotope Research Department of the Yerevan Physics Institute, which allows the proton beam to be ejected into the atmosphere. The design of the VW was created taking into account the requirements of scientists from different departments of the Institute.

The VM is equipped with an input collimator, which is also a fastening element to the output flange of the proton beam. A collimator with a 12 mm aperture is water-cooled. Because the vacuum in the system is $\sim 7 \times 10^{-6} - 10^{-7}$ mbar, the system must be cut off from the atmospheric pressure. For this, there is a special chamber after the collimator also with a 12 mm through-hole, and closed on both sides with stainless steel foils 50 microns thick. High purity helium flows between the foils for cooling. The beam loses about 1 MeV of energy in the foil so that users receive a beam with an energy of $\approx 16 - 17$ MeV at the output.

3. PROTON BEAM PROFILING STATION

The cyclotron proton beam profiling station consists of two VWMs. In the monitor for horizontal scanning, the vibrating wire is directed vertically, and for vertical scanning – horizontally. The feed-motion of monitors is done by linear actuators equipped with stepper motors. The components of the station are described in more detail below.

3.1. Main Parameters of Vibrating Wire Monitor

The principle of the VWM is to measure the natural frequency of a wire, which is highly dependent on the tension of that wire. The flux of particles falling on the wire causes the overheating of the wire, which influences its tension [17]. To excite stable oscillations of a wire at its natural frequency (or its harmonics), the interaction of the current flowing through the wire with a specially configured magnetic field based on strong permanent magnets with magnetic poles is used. The wire is attached at the input of the operational amplifier, which amplifies the emf from the wire during its random oscillations and supplies an amplified signal to the wire at the same phase. Such positive feedback results in the self-generation of natural oscillations of the wire because the quality factor of just such oscillations is maximum. The circuit is similar to the circuits for exciting oscillations of a quartz oscillator in many ways (for more details, see [18] and the literature cited there). The typical wire response times range from fractions of a second to several seconds, depending on the wire material and sensor size. The VWMs also have a strong thermal dependence concerning the temperature of the base on which the vibrating wire is attached. However, such dependence has much greater inertia, which makes it possible to select the useful signal from the wire quite simply.

Usually, to measure the beam profile (see, for example, [19]), we use the VWM operating at the second harmonic with two spaced sections of the magnetic field. This configuration frees up the beam scanning aperture located in the center of the wire. For the C18 cyclotron profiling station, two VWMs were manufactured with a new modification of the magnetic field, providing better flatness of this magnetic field. This flatness suppresses the excitation of the second harmonic of wire oscillations in a plane orthogonal to the plane of the magnetic gap and is slightly different from the required harmonic of oscillations in the plane of the magnetic gap. The general view of the monitor is shown in Fig. 1. To fasten the wire, a petal clamping system was used, made using an electric discharge machine. Heat-treated stainless steel (grade AISI 316 [20]) was chosen as the wire material. The length of the wires is 56 mm, the length of each section of the magnetic field along the wire is 10 mm, and the sensor aperture is 14 mm (see Fig. 1b).

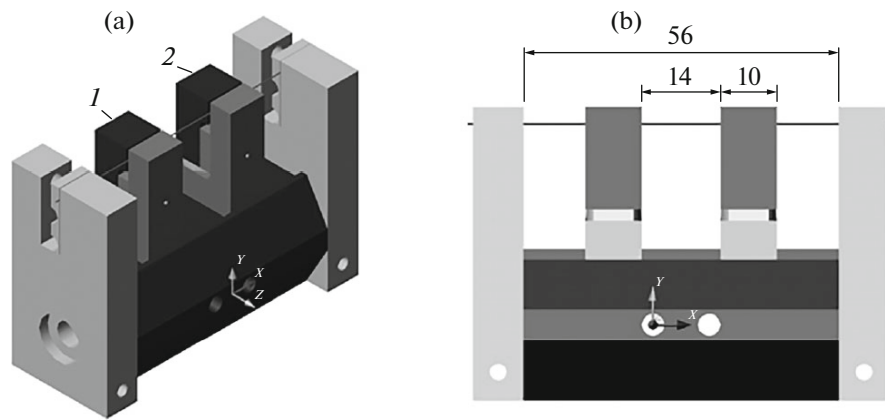


Fig. 1. General view of VWM: (a) the isometric view of the model, 1 and 2—modified system of magnetic poles, (b)—view along the beam axis with characteristic dimensions: monitor aperture 14 mm, the diameter of used permanent magnets 10 mm with a thickness of 3 mm.

3.2. Assembling the Profiling Station

A proton beam profiling station with two VWMs is assembled on a single platform. A steel square tube of $100 \text{ mm} \times 100 \text{ mm}$ was used as the supporting part of the monitor feed-motion system. On the horizontal and vertical surfaces of this tube, the linear drive mechanisms are mounted based on stepper motors with a positioning accuracy of 10 microns. Actuators are equipped with limit switches allowing also VWM park positioning. It was expected from preliminary considerations that the proton beam at the exit from the vacuum window has a sufficiently large divergence. Because the horizontal and vertical scanning monitors are spaced along the beam axis (Z -axis), the corresponding scans were supposed to be performed alternately from the side of the horizontal scanning monitor and then, after turning the profiling station by 180° around vertical axis from the side of the vertical scanning monitor.

3.3. Electronics System and Software

The advantage of VWM is that the output signal is a frequency signal generated by a specially designed autogeneration board, which ensures the excitation of stable oscillations of the wire at its natural frequency. For the profiling station, a special autogeneration board was used, made for the DW-VWM sensor, which contained two wires spaced by a screen [21]. This board contains a minimum of electronic components and is located near the monitor. In this case, the measuring/interface part of the electronics is carried out into the control room and is not exposed to radiation. The frequency nature of the transmitted signal allows one to use the conventional LAN cables for transmission with a length of up to 100 m. The unit is powered from the mains by the $\pm 12 \text{ V DC}$. To ensure the protection of the listed electronics assemblies from radiation and interference from the electromagnetic field, all electronics are placed in a metal box. The electronics system of the monitors also includes a frequency measurement board located in the control room, which contains an interface for communicating with a computer using a serial port. The oscillation autogeneration board and the measuring frequency board are connected by the LAN cable, the length of which in this experiment was $\sim 50 \text{ m}$. In this case, the measuring board was powered from the side of the autogeneration board by a $\pm 12 \text{ V DC}$. The oscillation excitation and frequency measurement boards were designed and manufactured by us. The stepper motor was controlled by standard drivers and also using a LAN cable.

The software is developed based on VisualBasic 2010. The program contains a universal window for visualizing the results, as well as modules for monitoring and controlling vibrating wire monitors and stepper motors.

4. EXPERIMENTS ON MEASURING THE PROTON BEAM PROFILE OF THE C18 CYCLOTRON

Taking into account the assumed large angular divergence of the beam, the profiling station of the proton beam launched into the air was installed at the minimum possible distance from the vacuum window.

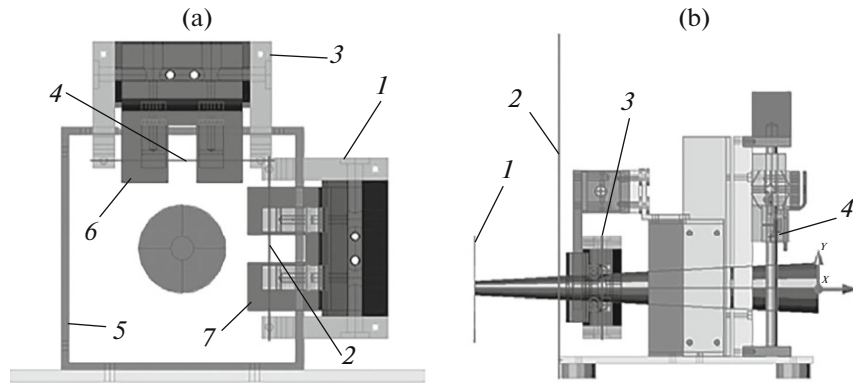


Fig. 2. View of the profiling station along the beam axis: (a) 1—VWM1 horizontal scanning with vibrating wire 2; 3—VWM2 vertical scanning with vibrating wire 4; 5—square tube; 6—lead protective plate. Side view of the station (b): 1—vacuum window collimator; 2—end panel of the metal box of the station; 3—VWM1; 4—VWM2.

A general view of the relative position of monitors and a proton beam with an angular divergence of 5° (assumed value) is shown in Fig. 2 (the monitors are located in park positions).

The distance between surfaces 1 and 2 is 62 mm, the distance between the wires VWM1 and VWM2 is 123 mm (along the beam axis). To protect the entire profiling system from convective air flows, as well as from radiation partially, the entire system is housed in a metal box with inlet and outlet holes for the beam. In addition, to prevent the accumulation of residual radiation on the monitors, the latter are protected by lead screens, which ensure that only the wires are exposed to the proton beam.

4.1. Horizontal Scanning of the Beam

In the first horizontal scanning experiment, two feed-motion rates were used, 0.2 mm/s and 1 mm/s. The ion current of the accelerator source was initially set to 38 mA, which corresponded to a beam current of $\sim 0.5\text{--}1.5\ \mu\text{A}$ (according to indirect measurements). A general view of the experimental data is shown in Fig. 3 (the dependence of the frequency and position of the VWM1 monitor on time).

During the third scan, there was a failure in reading responses from the stepper motor, and the monitor was brought to the park position by the “Reset” command without recording information about the monitor position.

Figure 3 shows the drift of the monitor frequency after turning on the beam, associated with significant heating of the monitor housing/protective lead screen (see below). It can be seen that the structure of the VWM1 frequency signal is generally the same for slow scans. The initial frequency upon contact with the beam begins to drop quite sharply owing to heating; however, upon leaving the beam (in Fig. 3 these are the minima of the frequency drop), a peak was observed on the frequency curve characterizing certain thermal processes in the wire, which revealed themselves on the back scan in the form of a bend on the slope.

Note that there was also a strong correlation between the frequencies of both monitors (VWM2 was in the park position all the time), and the noisiness of the frequency of the second monitor also correlates with the VWM1 position (see Fig. 4).

This correlation can be explained by the occurrence of thermal processes with a much longer delay time as compared to the characteristic response time of the wire, which for a given monitor is $\approx 0.46\ \text{s}$ (the computed time).

After horizontal beam scanning experiments, which also included raising the ion source current to 120 mA, the profiling station underwent a visual inspection and it was found that the lead screen protecting the magnetic components and the VWM1 base was indeed exposed to strong heat and even at the edge of the screen entry into the beam melted with the formation of a cavity (see below Fig. 11). It is clear that this heat with delay was transmitted to the base of the sensor and resulted in the observed drifts of the VWM1 frequency.

Let us consider the scanning process in the first part of the experiment in more detail (see Fig. 5, the time range is 10:48:00–11:11:00), in which we explain the structure of the frequency signal of VWM1.

Before switching on the high frequency (11:50), the noise of signals from both monitors was $\approx 0.01\ \text{Hz}$ (the Average Deviation function of the Excel program is 0.0094 and 0.011 Hz for the first and second

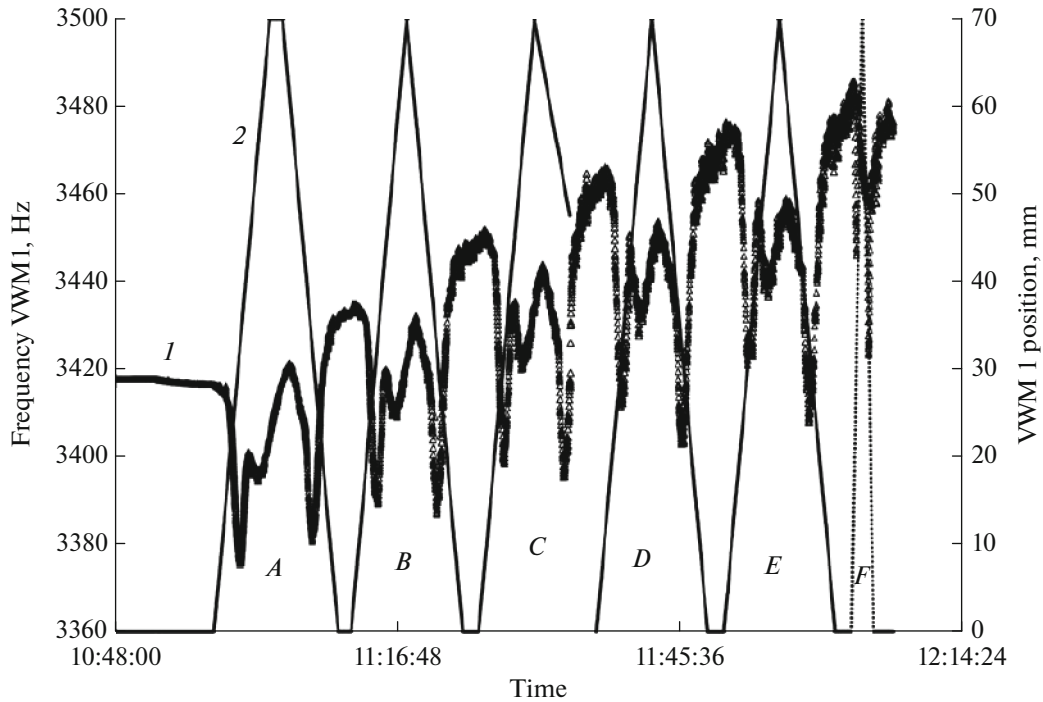


Fig. 3. Results of beam scan with the same beam current and two values of the scanning speed (in sections *A, B, C, D, E*—0.2 mm/s, in section *F*—1 mm/s.): *I*—VWM1 frequency, *2*—VWM1 position, *A, B, C, D, E, F*—areas of sequential scans.

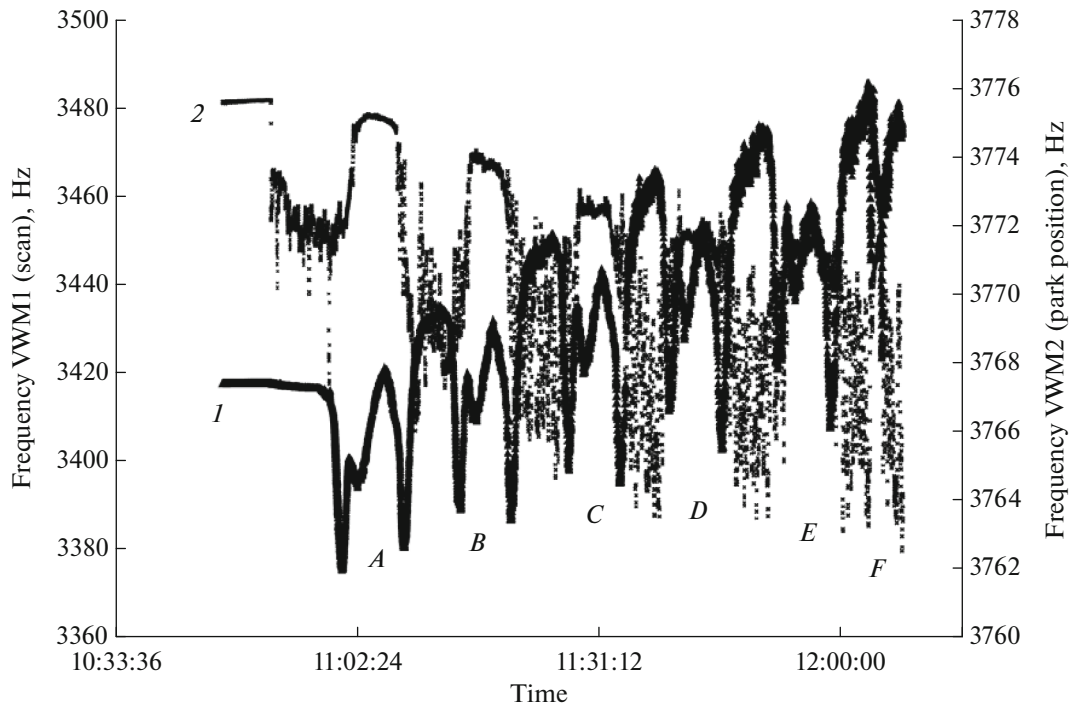


Fig. 4. Correlation between the readings of the VWM1 and VWM2 monitors: *I*—VWM1 frequency, *2*—VWM2 frequency, sections *A, B, C, D, E, F*—sequential scans.

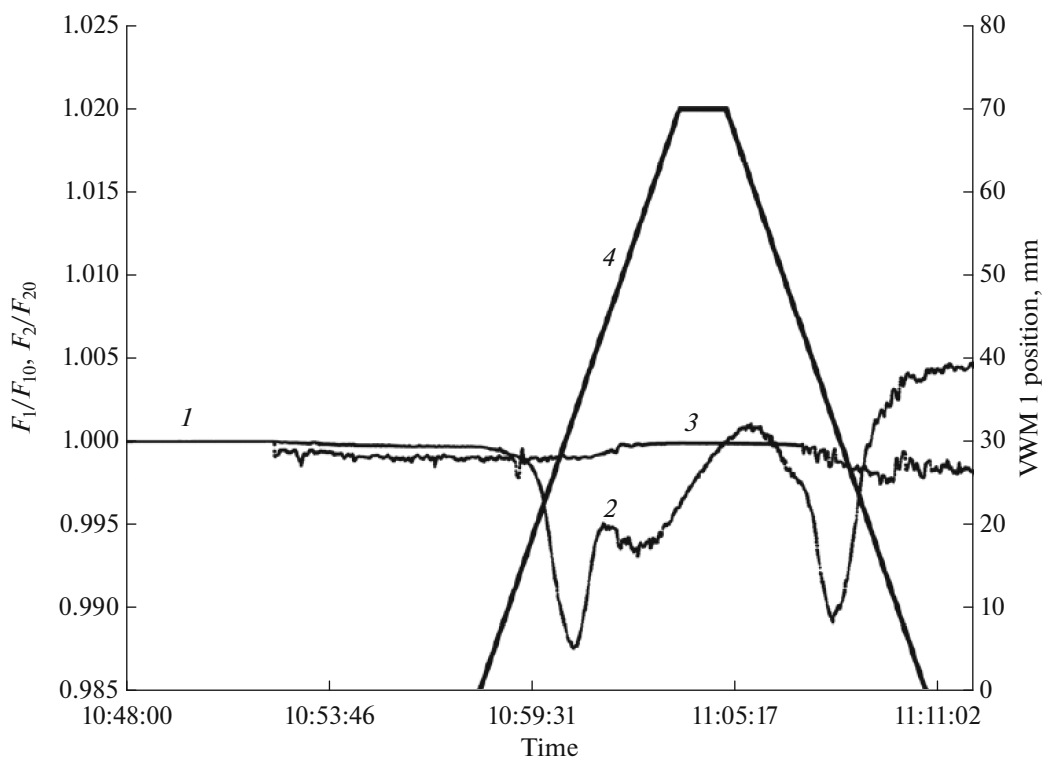


Fig. 5. Dependence of the relative frequencies VWM1 and VWM2 and the position of the first monitor on time (ion source current 38 mA, beam current 0.5–1.5 μA): 1—frequency section before switching on high frequency (HF) with a low noise level (in this section the signals VWM1 and VWM2 coincide), 2—a characteristic peak when the lead screen hits the beam, 3—the section of suppression of the frequency noise of the second monitor when the beam is fully exposed to the lead plate, 4—position of VWM1.

monitors, respectively) (1 in Fig. 5). The inclusion of high frequency significantly increased the noise of both monitors, and if for the first only up to 0.12 Hz, then for the second - up to 1.3 Hz. Hence it follows that a beam is formed at the exit of the cyclotron even without starting the ion source (due to the acceleration of the residual H^-). The scanning process started at 10:58:00. It can be seen from Fig. 5 that when leaving the beam in the forward direction of scanning, the frequency of both the first (scanning) and the second monitors were tuned. In this case, the characteristic position of the scanning monitor was ≈ 41 mm and corresponded to the beginning of the process of crossing the beam with the edge of the protective lead screen. The heat dissipation of the power transmitted from the side of the beam at the edge was small, and the edge began to melt. At the same time, the noise level of the VWM2 frequency signal dropped significantly and amounted to only 0.015 Hz (the VWM1 monitor was at the 70 mm position, section 3 in Fig. 5).

In the second session of the experiment, two scans were performed at an ion source current of 60 and 100 mA. Then the monitor was moved to the position of 30 mm (the value corresponding to the maximum effect of the beam on the wire frequency), at which the value of the ion current changed stepwise according to the following values of the ion source current: 40, 50, 60, 70, 80, 90, 100, 110, and 120 mA. At the end of this series of values, VWM1 was parked and a full scan was performed to a depth of 70 mm at an ion current of 120 mA (see Fig. 6).

As in the first session, we choose the beginning of the experiment for analysis (see Fig. 7), because during subsequent scans, as noted above, the beam hit the lead screen and the sensor base was overheated, which is accompanied by a frequency drift.

As in Fig. 5, there is a decrease in the noisiness of the VWM2 frequency signal at a VWM1 scanning depth of more than 40 mm.

To reconstruct the horizontal profile of the beam, we will choose this scanning, because the long-term irradiation of the protective lead plate VWM1 has just begun here and the thermal drift of the frequency is still moderate. Figure 8 shows the dependences of the relative frequencies VWM1 and VWM2 (normalization to the frequency in the park position VWM1).

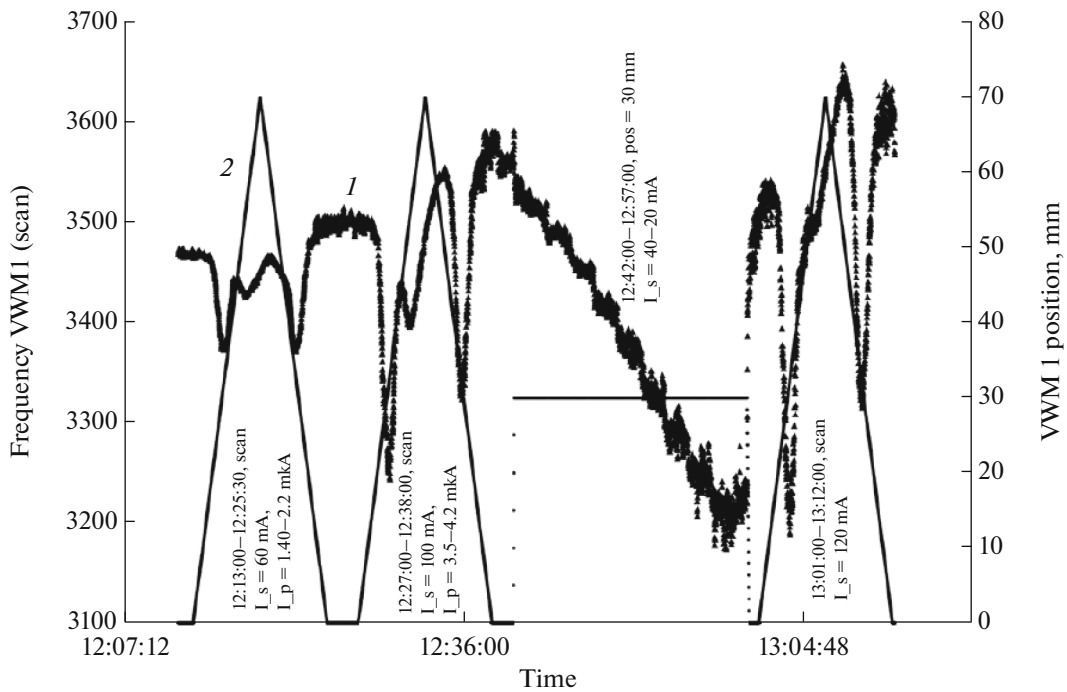


Fig. 6. Results of horizontal scanning in the second session of the experiment. Time dependence of frequency and position of VWM1. 1—VWM1 frequency, 2—VWM1 position.

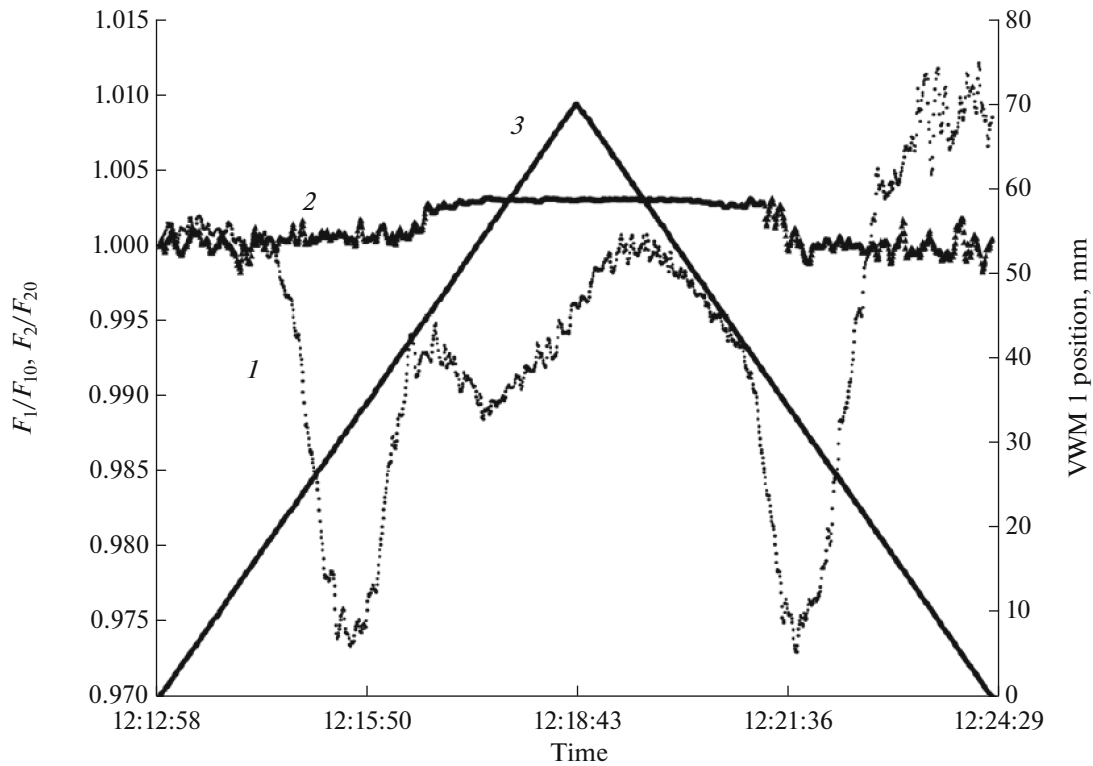


Fig. 7. Dependence of the relative frequencies VWM1 and VWM2, as well as the position of the first monitor, on time at the beginning of the second session of the horizontal scanning experiment (ion source current 60 mA, beam current $\sim 1.4-2.2 \mu\text{A}$). 1—VWM1 signal, VWM2 signal, 2—VWM1 position.

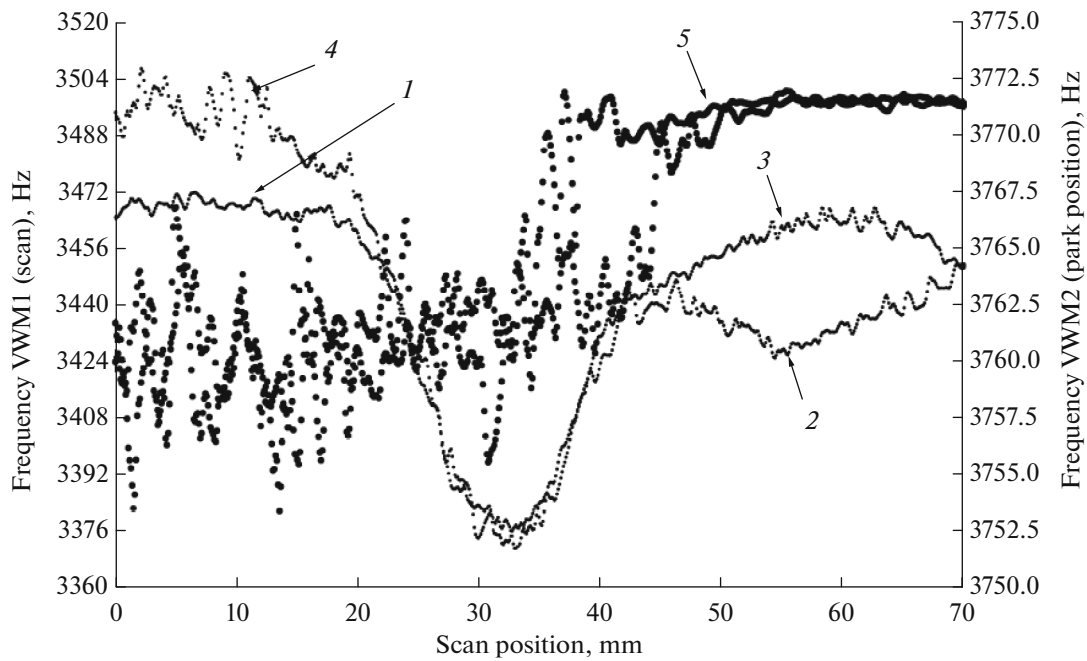


Fig. 8. Dependences of the VWM1 and VWM2 relative frequencies on the VWM1 position (ion source current 60 mA, beam current $\sim 1.4\text{--}2.2\ \mu\text{A}$). Arrows indicate 1—the start of forwarding scanning (towards increasing values of VWM1 positions), 2—frequency behavior after VWM1 hits the lead plate edge, 3, 4—frequency behavior during back scanning, 5—VWM2 frequency.

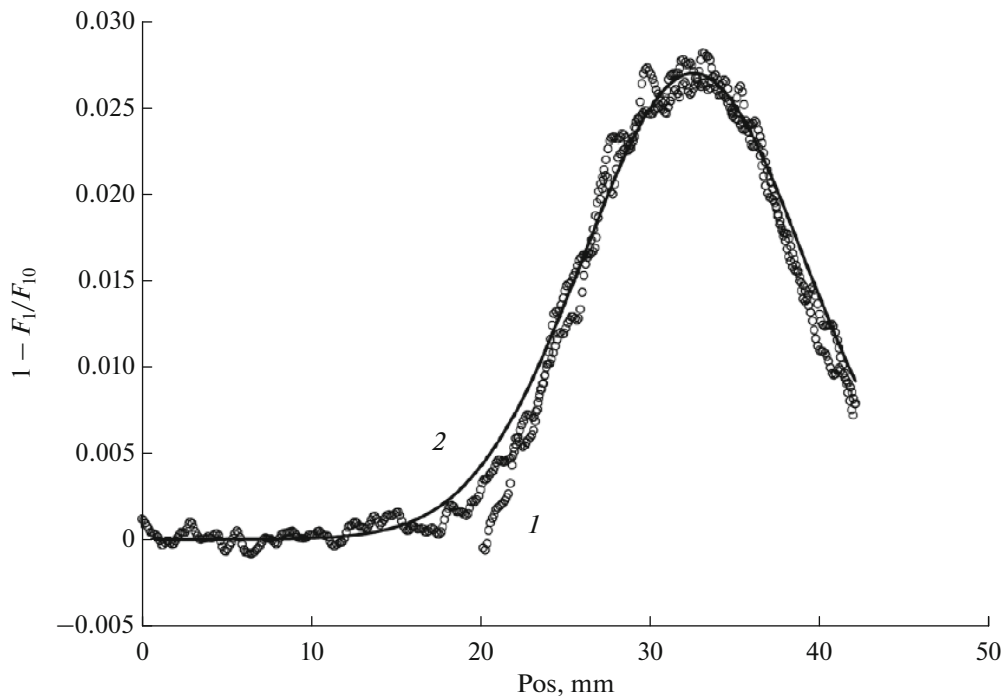


Fig. 9. Reconstruction of the horizontal beam profile for current source energy of 60 mA. 1 (circles)—experimental data within 12:13:00–12:25:00, 2 (solid line)—fitting to the Gaussian curve.

To reconstruct the beam profile, the points corresponding to the beginning of the forward scan and beam scanning up to the VWM1 position of 42 mm were selected, as well as the points of the back scan from the 42 mm position to 20 mm. These experimental points were used to fit the Gaussian curve (see Fig. 9).

Typical parameters of the Gaussian profile: center of the curve 32.5 mm, standard deviation 6.5 mm.

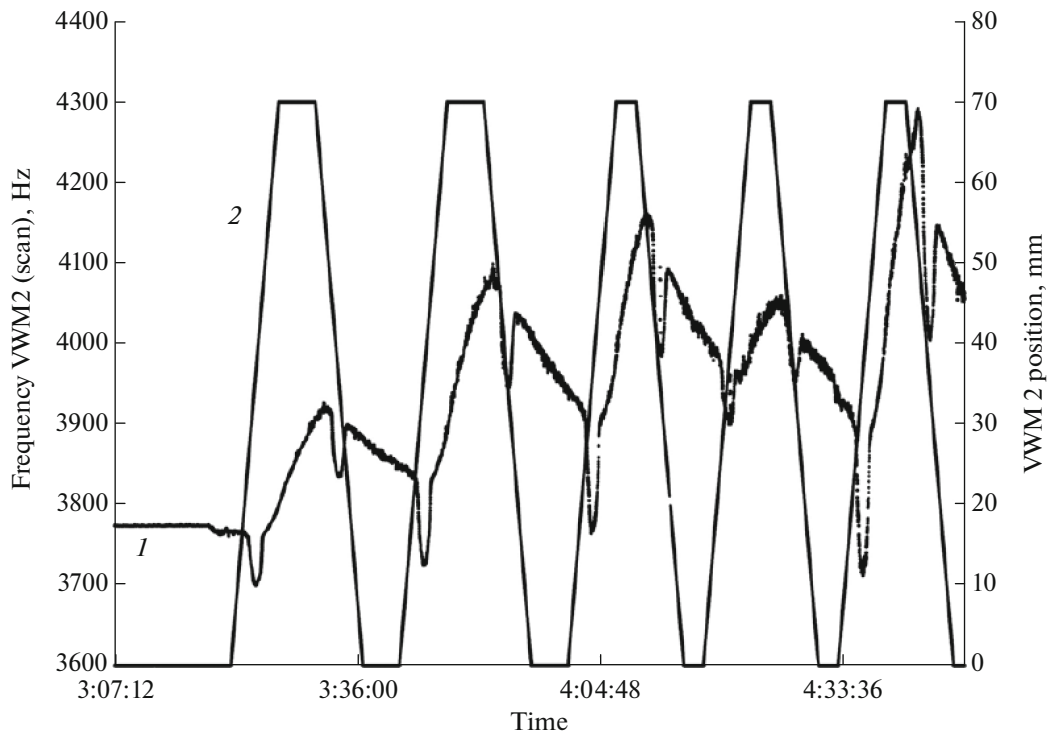


Fig. 10. General view of data on vertical beam profiling: dependence of VWM2 frequency and monitor position on time. 1—ion beam current 90, 2—100, 3—110, 4—70, and 5—120 mA.

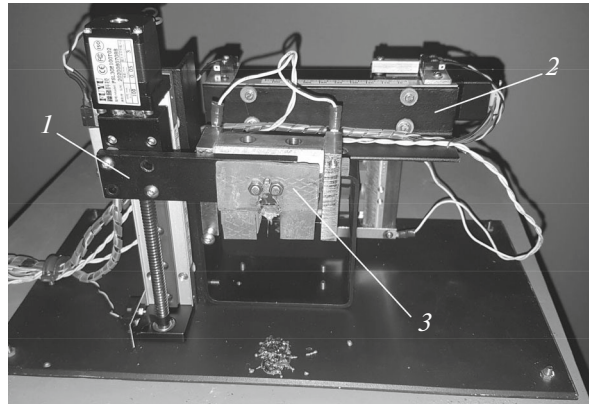


Fig. 11. View of the vertical scanning monitor after the end of the experiment: 1—(in the foreground) vertical scanning monitor, 2—(in the background) horizontal scanning monitor, 3—melted protective screen VWM2.

4.2. Vertical Scanning of the Beam

Vertical scanning was carried out three weeks after horizontal scanning because according to the experiment scenario, the profiling station should be turned 180° around the vertical axis so that VWM2 should be exposed to the beam, and scanning should be performed along the same section as horizontal scanning (section plane at a distance of 62 mm from the surface vacuum window). To do this, it was required to wait until the background radiation of the profiling station reaches an acceptable level. A general view of the experimental data is shown in Fig. 10 (dependence of the frequency and position of the VWM2 monitor on time). A total of five scans were performed at a total depth of 70 mm at various proton beam currents. Because the beam current was measured indirectly and inaccurately, we present the corresponding values of the ion source of the beam: 90, 100, 110, 70, and 120 mA.

As it was clarified from the experiments on horizontal scanning, the monitor in the process is exposed to considerable thermal influence. Fig. 11 presents VWM2 after the end of the series of scans (the picture was taken two weeks after the end of the experiment).

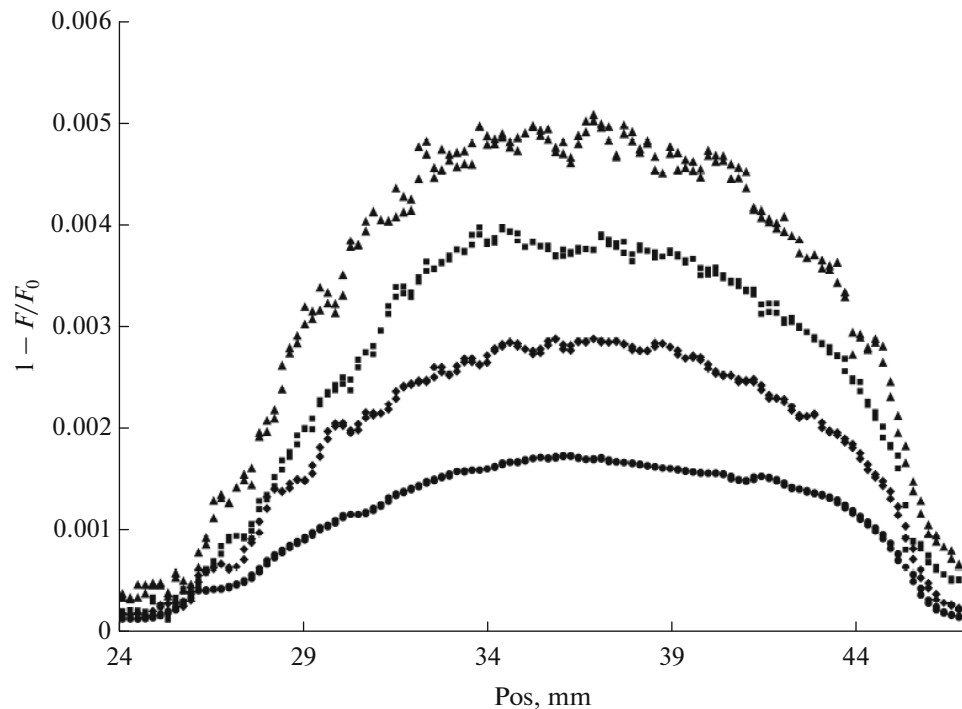


Fig. 12. Vertical beam profiles for different beam currents. From bottom to top, the current of the ion source corresponds to the values: 90, 100, 110, 120 mA.

It can be seen that just as for horizontal scanning at large monitor displacements, the significant heat transfer occurs from the side of the proton beam to the protective lead plate, up to its melting. On which of the scans this happened, unfortunately, this is not visible according to the results of the experiment. It can be seen, however, that the sensor in all cases remained operational both when scanning down (moving from park position) and when moving up (returning to park position). However, to reconstruct the beam profile due to the strong thermal drift after the lead plate hits the beam, it is preferable to use the data only when scanning down to a value of 24–25 mm.

Figure 12 shows the corresponding beam profiles in this range for the ion source current values: 90, 100, 110, 120 mA. As the information on the beam profile, we used the function $1 - F_2/F_{20}$, where F_2 is the current measured frequency VWM2, F_{20} is the frequency value at the position of 20 mm (before the entry of the wire into the beam).

As can be seen, the beam is far from the Gaussian distribution at all values of the beam current. Nevertheless, we present the fitting of the experimental points of the Gaussian curve (Fig. 13).

The characteristic parameters of the Gaussian profile: the center of the curve is 37 mm, the standard deviation is 6.5 mm.

5. CONCLUSION

The experiments have shown the efficiency of all the units of the profiling station including the two-channel oscillation autogeneration board, the system of linear drives for horizontal and vertical scanning monitors. The connection between the experimental room and the control room also functioned satisfactorily. The frequency measurement and computer interface board ensured reliable communication with the monitors and stepper motors of linear actuators. Both monitors have shown performance in rather severe conditions of strong overheating of protective lead plates. For all values of the proton beam current, the oscillations of the wires of both monitors were not disrupted. For the first time, all this made possible the measurements of the horizontal and vertical profiles of the proton beam at the exit from the vacuum window.

The shortcomings of the profiling station were also discovered. First of all, these concerns monitors, which had an insufficient aperture and short clips that clamp the wire. The protective lead plates were cut to an insufficient depth along the scanning axis. All this results in their exposure to a proton beam and the appearance of

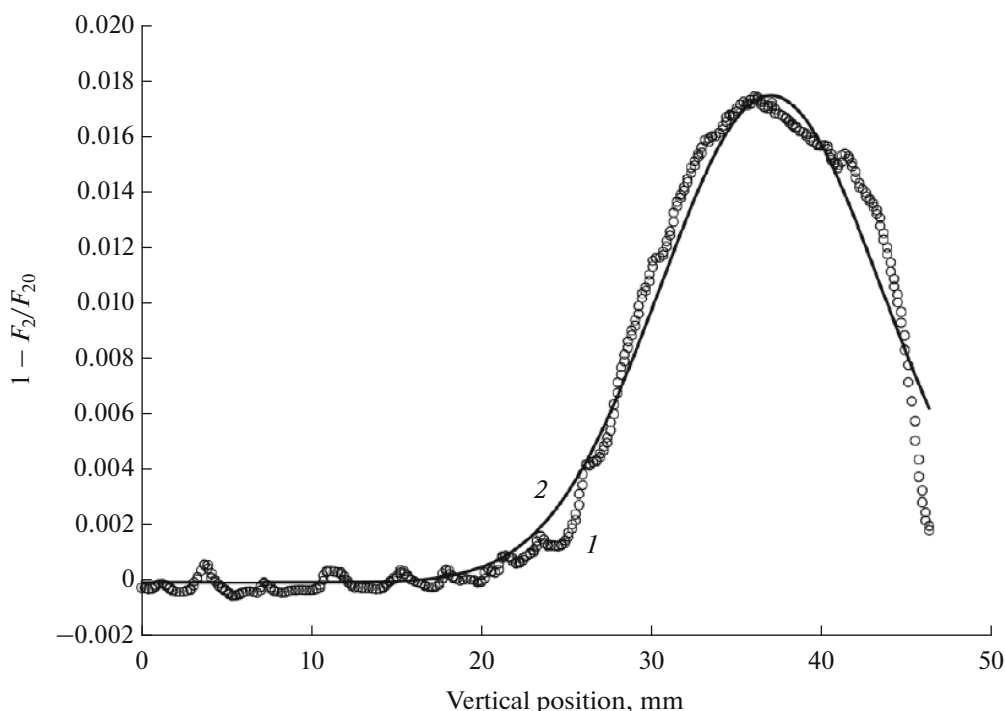


Fig. 13. Reconstruction of the vertical beam profile for current source energy of 90 mA. 1 (circles)—experimental data within 15:21:01–15:26:41, 2 (solid line)—fitting to the Gaussian curve.

noise caused by strong heat release. The problem of synchronizing the frequency measurements with the signals of the monitor position during scanning caused by the use of computer time signals was also noticed. For slow scans, this problem is not significant but can result in inaccuracies during fast scans.

To equip the C18 cyclotron with a standard profiling station the monitors with an enlarged aperture should be used (it seems that 20 mm will be sufficient). The clips of the wire should be lengthened so that the beam can freely exit into the area between the wire and the base of the monitor. The use of protective lead plates was advisable, however, it would be more correct to make a cutout in the plate strictly along the contour of the projection of the base and the magnetic system of the monitor. In this case, it is more convenient to use flat plates and provide on the base of the monitor for fixing the plate with screws located as far as possible from the scanning axis. When carrying out scanning, it is advisable not to scan to a fixed maximum depth, but to use feedback on the frequency drop of the monitors and stop moving when the wire leaves the beam. It is also advisable to reduce the distance between the sections of horizontal and vertical scans, and with the use of linear drives with a sufficient range of motion — combine these planes. When performing scans, the system for measuring the total beam current should be started, which will make it possible to obtain the beam profiles in absolute units of current density along the scanning axis. In the new electronics modification, it is advisable to provide a board for control and registration of frequency signals and stepper motors with own timer.

ACKNOWLEDGMENTS

The authors express their sincere gratitude to A. Avetisyan for supporting this work at its initial stage.

FUNDING

The study was carried out with the financial support of the Science Committee of the Republic of Armenia within the framework of the Scientific Project 20APP-2G001.

CONFLICT OF INTEREST

The authors declare no conflict of interest.

REFERENCES

1. <https://www.iba-radiopharmasolutions.com/cyclotrons>.
2. <https://www.iba-radiopharmasolutions.com/radioisotopes>.
3. <https://www.petct-armenia.am/>.
4. Karamysheva, G.A., Karamyshev, O.V., Kostromin, S.A., Morozov, N.A., Samsonov, E.V., Syresin, E.M., Shirkov, G.D., and Shirko, S.G., *Technical Physics*, 2012, vol. 57, no. 1, p. 106.
5. Jasna, L., *PRST, AB*, 2001, vol. 4, p. 123501.
6. Kleeven, W., Forton, E., Kral, E., Nactergal, B., Nuttens, V., Van de Walle, J., and Zaremba, S., *IBA*, Louvain-la-Neuve, Belgium, Proceedings of Cyclotrons, Zurich, Switzerland, 2016.
7. Avagyan, R.H., Avetisyan, A.E., Kerobyan, I.A., and Taroyan, S.P., *J. Contemp. Phys.*, 2009, vol. 44, p. 250.
8. Agababyan, K.Sh. and Demekhina, N.A., Preprint EFI -823(50)-85, (1985).
9. Sirunyan, A., Hakobyan, A., Ayvazyan, G. et al., *J. Contemp. Phys.*, 2018, vol. 53, p. 271.
10. Sirunyan, A.M., *Development of experimental methods and research in nuclear physics on the YerPhI injector and elementary particles in international centers* (CERN-LHC, DESY-H1, JINR), <http://www.ru.convdocs.org/docs/index-235948.html>.
11. Kerobyan, I. and Marukyan, H., *J. Contemp. Phys.*, 2020, vol. 55, p. 8.
12. INTERNATIONAL ATOMIC ENERGY AGENCY, *Cyclotron Based Production of Technetium-99m*, Radioisotopes and Radiopharmaceuticals Reports No. 2, IAEA, Vienna (2017).
13. Avetisyan, A. et al., *EPJ Web of Conferences*, 2015, vol. 93, p. 08001.
14. Avetisyan, A., Sargsyan, R., Melkonyan, A., Mkrtchyan, M., et al., *IJESIT*, 2015, vol. 4, no. 3, p. 37.
15. <https://www.iba-radiopharmasolutions.com/cyclotrons-equipment>.
16. <https://www.elexcomm.com/product/539d84643beb6ec14b00000d>.
17. Arutunian, S.G., Mailian, M.R., and Wittenburg, K., *NIMA*, 2007, vol. 572, p. 1022.
18. Arutunian, S.G., Margaryan, A.V., Harutyunyan, G.S., Lazareva, E.G., Chung, M., Kwak, D., and Gyu-lamiryan, D.S., *JINST*, 2021, vol. 16, p. 1.
19. Aginian, M.A., Arutunian, S.G., Choe, D., Chung, M., Harutyunyan, G.S., Kim, S.-Y., Lazareva, E.G., and Margaryan, A.V., *J. Contemp. Phys.*, 2017, vol. 52, p. 110.
20. <http://www.goodfellow.com/catalogue/GFCatalogue.php?Language=E>.
21. Chung, M., Arutunian, S.G., Harutyunyan, G.S., Kwak, D., Lazareva, E.G., Margaryan, A.V., and Tumanyan, M.A., *8th International Beam Instrumentation Conference, IBIC2019*, Malmo, Sweden, Malmo, Sweden, 2019, p. 368.

Translated by V. Musakhanyan